Temperature-Resolved Surface Infrared Spectroscopy of CO on Rh(111) and ( $2\times1$ )-O/Rh(111)

Elizabeth A. Jamka, Maxwell Z. Gillum, Christina N. Grytsyshyn-Giger, Faith J. Lewis, and Daniel R. Killelea\*

Department of Chemistry & Biochemistry, Loyola University Chicago, 1068 W. Sheridan Road, Chicago, Illinois 60660, United States

Email: dkillelea@luc.edu

Phone: +1 (0)773 508 3136

### **Abstract**

Heterogeneously catalyzed reactions over transition metal surfaces in a pillar of chemical industry and accounts for a significant fraction of the global energy demand. CO oxidation provides insight into the relative reactivity of various oxygenaceous surface phases, and it is necessary to first understand where it binds to the surface and the nature of the local environment to develop robust mechanistic pictures of the reaction. Surface IR spectroscopy is a quantitative technique that also provides information about the binding sites and chemical environments of the adsorbed CO molecules. Here, we report results from a study of CO sticking to clean Rh(111) and (2×1)-O/Rh(111) that shows that the intensity of the IR absorption was not linear with coverage and is an important consideration for further study of the catalytic surface.

### I. Introduction

The oxidation of small molecules over metal surfaces is of widespread importance in heterogeneous catalysis.<sup>1-3</sup> In particular, the oxidation of carbon monoxide (CO) to carbon dioxide (CO<sub>2</sub>) has attracted much interest because it is relevant to industrial and consumer processes (e.g., catalytic converter in automobiles) and also because it allows for the study of the surface species because of the lack of molecular complexity.<sup>4, 5</sup> CO oxidation has been studied using a variety of techniques including molecular beam surface reactive scattering, 6-8 temperature programmed desorption/reaction (TPD/TPR) to monitor the production of CO<sub>2</sub>, 9-13 X-ray Photoelectron Spectroscopy (XPS) to speciate the surface species through the reaction via elemental analysis, and Reflection-Absorption Infrared Spectroscopy (RAIRS), which provides molecular information about the surface adsorbates. 14-17 Together, a picture has emerged about the surface-catalyzed oxidation of CO on a variety of different metal surfaces, but as key details are discovered, there is an emerging consensus that this seemingly 'simple' reaction is far more complicated than was thought even a few years ago.7, 18, 19 In particular, recent discoveries showing that surface oxide reactivity is strongly correlated to geometry<sup>20</sup> and that terrace and steps proffer very different catalytic activities, 7, 21 has spurred us to study the different oxygenaceous phases on Rh(111), where we have developed robust approaches for preparing three distinct phases.<sup>22-24</sup> Here, we present results showing that even CO adsorption to clean Rh(111) has complexities that must be considered in order to properly use RAIRS to determine the species present and their coverages.

The IR absorption spectrum of adsorbed CO is sensitive to the binding site and thus has been used to qualitatively probe the state of the surface through the sensitivity of the main CO stretch frequency to metals.<sup>25, 26</sup> Although CO spectroscopy is well-developed, there have been only a handful of IR studies of CO on Rh(111) <sup>16, 27, 28</sup> and even fewer investigating CO on oxygenated Rh(111) surfaces.<sup>16, 29</sup> We have determined the chemical significance of various oxygen phases on different Rh surfaces,<sup>9, 10, 22-24</sup> and here, we have studied CO adsorption on Rh(111) and (2×1)-O/Rh(111). Studying CO oxidation on different Rh surfaces provides atomic level information regarding oxidation reactions, progressing the understanding of various surface phases relevant to many Rh catalyzed processes.

O<sub>2</sub> readily dissociates on Rh(111) to form adsorbed oxygen (O<sub>ad</sub>), and adsorption is kinetically limited to an oxygen coverage ( $\theta$ c) of 0.5 monolayers (ML, 1 ML = 1.6 ×10<sup>15</sup> atoms cm<sup>-2</sup>).<sup>9, 30, 31</sup> CO does not dissociate on Rh(111) and chemisorbs as an intact molecule. CO preferentially adsorbs on atop sites and arranges in a ( $\sqrt{3}$ × $\sqrt{3}$ )R30°-CO adlayer with a CO coverage ( $\theta$ co) of 0.33 ML CO. Upon continued exposure, CO adsorbs to bridge sites as well and reaches  $\theta$ co = 0.75 ML in a (2×2)-3CO structure.<sup>4, 16, 32</sup> The CO stretch for CO in atop sites has an absorption peak calculated and observed between 2015 cm<sup>-1</sup> and 2100 cm<sup>-1</sup>, depending on  $\theta$ co.<sup>16, 27</sup> On oxygenated surfaces, CO remains bound atop, while O occupies the hollow sites,<sup>16</sup> and the CO stretch was observed to increase by ≈ 25 cm<sup>-1</sup> to 2085 cm<sup>-1</sup>.<sup>16</sup> However, it is important to note, that the previous IR measurements were typically made at low-temperature (T<sub>exp</sub> < 200 K) and it does not

seem that the behavior of the IR spectra with respect to temperature has been investigated.

In this paper, RAIRS and TPD were employed simultaneously to determine both the CO coverage on the surface and the binding sites and chemical environment for CO on Rh(111). The combination of TPD and RAIRS provides the chemical species and their local environment over a range of surface temperatures and adsorbate coverages. With the behavior of CO on clean Rh(111) established, the adsorption of CO to an oxygenated Rh(111) surface, the ( $2\times1$ )-O structure, was studied over a range of temperatures during a TPD experiment. In both cases, we observed that the IR peak shifts in accordance with previous measurements, but the intensity varies and is most intense, on a per-molecule basis, at low coverages. This suggests that the intensity of the absorption for the CO stretch does not linearly depend on  $\theta_{CO}$ , meaning that correlation of  $\theta_{CO}$  to the RAIRS signal requires more than a simple application of Beers Law to the IR spectra.

# II. Experiment

All experiments were performed in an ultra-high vacuum (UHV) system described previously.<sup>24</sup> The system is comprised of two connected chambers, a preparation chamber (base pressure of 1×10<sup>-10</sup> Torr) and a scanning tunneling microscope (STM) chamber (base pressure of <2×10<sup>-11</sup> Torr). The preparation chamber was equipped with multiple surface science techniques including a Specs ErLEED 150 with 3000D controller (LEED), a PHI 10-155 Meitner-Auger Electron Spectrometer (MAES), and a Hiden HAL 3F 301 RC quadrupole mass spectrometer (QMS) for temperature programmed desorption (TPD) analysis. RAIRS measurements were made with a Bruker FT-IR Invenio

R spectrometer and an external liquid nitrogen cooled MCT (mercury-cadmium-telluride) detector which increased sensitivity to around 800 cm<sup>-1</sup>. The IR light was p-polarized and traveled through enclosures purged with dry, CO<sub>2</sub> free air (Parker, Spectra30, FT-IR Purge Gas Generator). The RAIRS spectra are an average of 36 scans were taken with a resolution of 4 cm<sup>-1</sup> and new background spectra was taken at the start of each experiment. In some of the spectra on Rh(111), a small spurious background absorption peak, likely from adsorbed CO from the chamber background, was present when the IR background was obtained. This resulted in a negative peak in the ΔR/R or absorbance spectra around 2025 cm<sup>-1</sup> that appeared after CO exposure began and remained even after CO was desorbed. The small intensity and far-red shift indicated that this was only a small amount of CO. When present, this was removed from the spectra by taking CO stretch portion of the spectrum at high temperature, where the surface was clear of CO, inverting it, and adding it to all the spectra collected in that trial. This peak was never observed on the oxidized surface.

The Rh(111) crystal (Surface Preparation Labs, Zaandam, The Netherlands) sample was a 10 mm diameter disc and 3 mm thick and was mounted on an exchangeable tantalum (Ta) sample plate with a type-K thermocouple welded to the side of the crystal. The crystal could be cooled with liquid nitrogen loop to 100 K and heated using electron beam heating to 1400 K. The surface was cleaned with repeated cycles of Ar+ sputtering and annealing at 1300 K until the surface cleanliness was verified with a clean (1×1) LEED pattern and O<sub>2</sub> TPD free of CO<sub>2</sub>.

The Rh(111) sample was dosed with CO with a pressure of  $1\times10^{-6}$  Torr at an exposure temperature ( $T_{exp}$ ) of 300 K. For the oxidized surface, the Rh(111) was first dosed with O<sub>2</sub> by backfilling to  $1\times10^{-6}$  Torr for 60 s at  $T_{exp}=300$  K to yield a saturated surface with the adsorbed O (O<sub>ad</sub>) in a (2x1)-O adlayer and  $\theta_0=0.5$  monolayers (ML, 1 ML =  $1.6\times10^{15}$  atoms cm<sup>-2</sup>). After oxygen preparation, the surface was then separately dosed with CO at  $1\times10^{-6}$  Torr at  $T_{exp}=300$  K. Spectra were obtained both during CO exposure to measure uptake and during the TPD experiment to complement the QMS desorption measurements. Spectra between 850 and 4000 cm<sup>-1</sup> with a resolution of 4 cm<sup>-1</sup> were collected every 10 s. For the TPD experiments, QMS and RAIRS spectra were collected synchronously. The TPD was run from 100 K to 600 K with a ramp rate of 0.4 K s<sup>-1</sup>. CO oxidation on Rh(111) was complete by 600 K. The Rh(111) crystal was then annealed to 1250 K in between experiments to restore surface cleanliness and order, as verified with LEED.

### III. Results and Discussion

In order to use the IR spectra to quantify &<sub>O</sub>, it was first necessary to establish &<sub>O</sub> as a function of CO exposure at  $T_{exp}$  = 300 K. Figure 1A shows the TPD spectra taken after several CO exposures, clearly demonstrating the surface saturation after  $\approx$  15 Langmuir (L) CO exposure. The TPD spectra were background subtracted (as shown in Figure 1A) and then integrated to obtain &<sub>O</sub> using the known saturation coverage of CO on Rh(111) of &<sub>CO</sub> = 0.75 ML CO, $^{32}$  the CO uptake is shown in Figure 1B with the integrated TPD desorption in red on the left and the calculated &<sub>CO</sub> in blue on the left plotted with respect to the CO exposure in L.

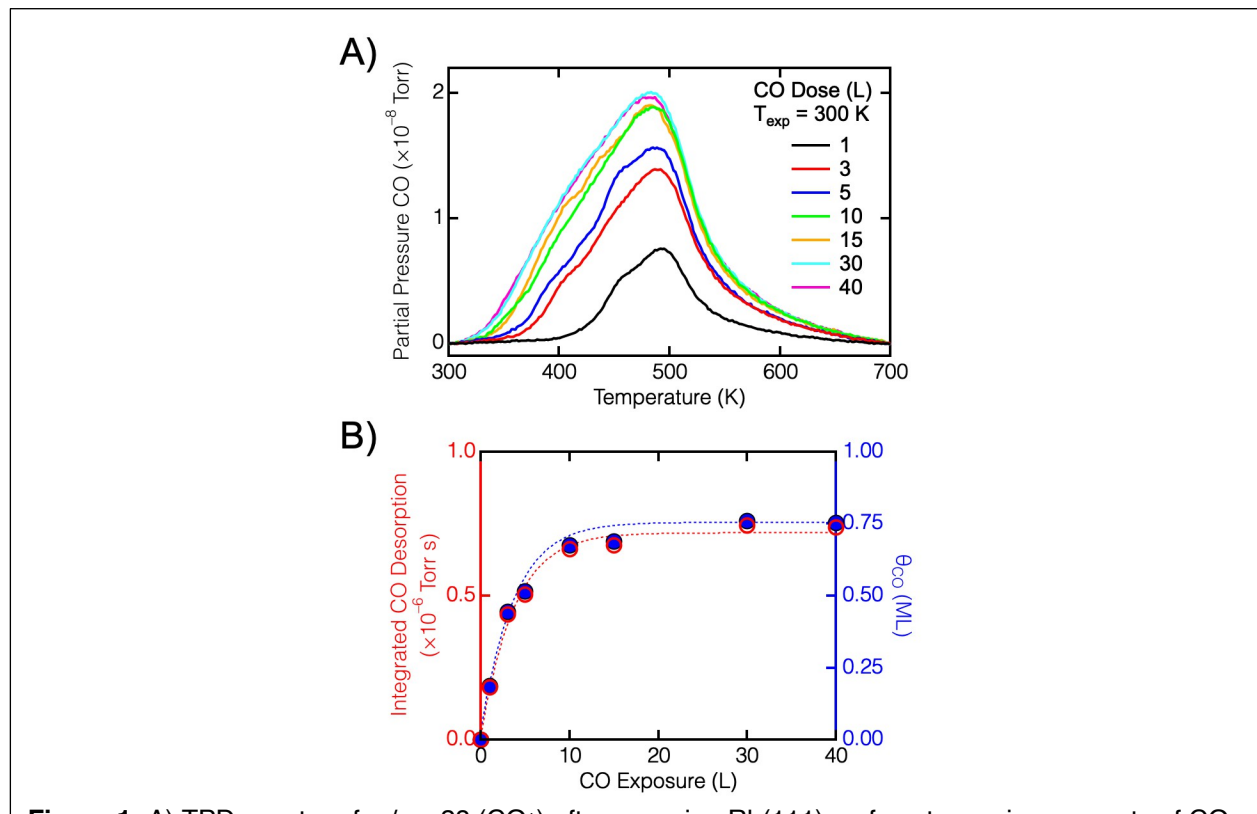


**Figure 1:** A) TPD spectra of m/z = 28 (CO+) after exposing Rh(111) surface to varying amounts of CO at  $T_{exp}$  = 300 K. Initial coverages are  $\theta_{CO}$  = 0.19 ML (—), 0.45 ML (—), 0.52 ML (—), 0.67 ML (—), 0.69 ML (—), and 0.75 ML (—). The heating rate was 4 K s<sup>-1</sup> for TPD. B) Integrated TPD area showing the uptake of CO at varying exposures and correlation between integrated desorption (red open circles, left) and  $\theta_{CO}$  (blue filled circles, right)

With the uptake quantified, the correlation between the RAIRS and &0 could be determined. Figure 2A shows RAIRS obtained after each of the CO exposures at  $T_{exp}$  = 300 K, in Figure 1A. Curiously, the highest peak was observed at 2072.2 cm<sup>-1</sup> after a 1 L CO exposure, &0 = 0.19 ML, and continued exposure saw the peak steadily redshift to 2084.2 cm<sup>-1</sup>, broaden slightly, and diminish in amplitude. As coverage was determined from the TPD spectra, it is not the case that CO was desorbing at 300 K for the longer CO exposures. Instead, it is more likely that the increased coverage decreased the permolecule IR absorption cross-section as the electron density available from the metal decreased, and the C–O bond strength increased, as suggested by the blue shift in the CO stretching absorption feature. The net result is that this seemingly anomalous

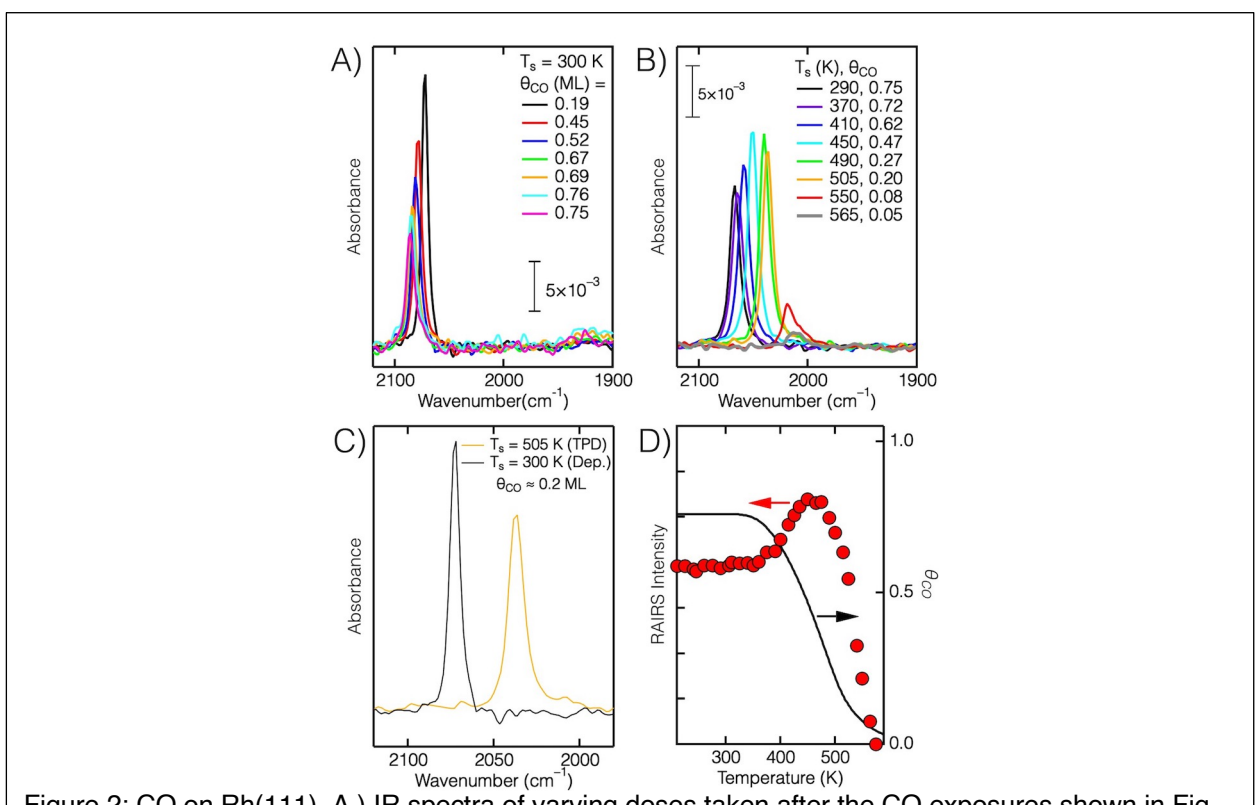


Figure 2: CO on Rh(111) A.) IR spectra of varying doses taken after the CO exposures shown in Fig. 1 at  $T_s$  = 300 K. B.) Sequence of the IR scans taken through TPD experiment with  $\theta_{CO, initial}$  = 0.75 ML. These show the decreased intensity and red shift in the CO absorption peak as temperature increased and  $\theta_{CO}$  decreased. C) The difference in IR spectra for similar coverages ( $\theta_{CO} \approx 0.2$  ML) collected after a 1 L CO dose at 300 K (—) and during the TPD experiment when  $\theta_{CO}$  has deceased from 0.76 ML (—), collected at 505 K. All RAIRS plots have the same vertical range,. D) RAIRS intensity (left)  $\theta_{CO, initial}$  = 0.75 ML during TPD experiment (red circles) and  $\theta_{CO}$  from TPD data (right, —).

behavior is indicative of a shift of electron density from the CO–metal bond to the CO molecule. Although this could be rationalized by 'back-bonding' where the metal contributed electron density to the  $2\pi^*$  antibonding orbital in CO, the situation is probably more complex, but the result the same.<sup>33-35</sup> Above  $\theta_{\text{CO}} \approx 0.6$  ML, this effect diminished and the peak intensity remained constant, while still modestly blue-shifting.

The convoluted relationship between absorption frequency and peak intensity was also present when surface temperature ( $T_s$ ) increased concomitantly with a decrease in  $\theta_{CO}$ , as shown in the RAIRS collected during the TPD experiment in Figure 2B after a 30 L CO dose at  $T_{exp} = 300$  K and  $\theta_{CO,initial} = 0.75$  ML. With increasing  $T_s$ , and thus decreasing

 $\theta_{CO}$ , the C-O stretch frequency red-shifted, suggesting strong CO-metal bond and weakening C-O bond, while the intensity does not appear to decrease linearly with  $\theta_{CO}$ . The observation of a pronounced increase in intensity for the absorbance of the C-O stretch was robust, as it was observed with isothermal uptake at  $T_{exp} = 300$  K and during the TPD experiment where  $T_s \approx 500$  K; the spectra for similar  $\theta_{CO}$  for the two different paths is shown in Figure 2C. Although we are unable to state definitely why the absorption frequencies differ, it is reasonable to assume that the shift is caused by the difference in  $T_s$  for the two spectra. This effect is also evident in Figure 2D for a 30 L CO dose at  $T_{exp}$ = 300 K, and  $\theta_{CO, 1}$  = 0.75 ML, where the black trace (right axis) is  $\theta_{CO}$  from the TPD measurement and the red circles (left axis) is the integrated intensity of the C-O stretch peak (between 2072 cm<sup>-1</sup> and 2086 cm<sup>-1</sup>) in the RAIRS data. As shown, despite a roughly 50% decrease in  $\theta_{CO}$ , the integrated intensity of the CO stretch peak actually increased. With additional desorption the RAIRS signal did diminish, but at the point where  $\theta_{CO}$  was down to 25% or so of the original value. It is important to note that the  $\theta_{\rm CO}$  from the TPD measurement was an upper limit, and most likely exceeded the actual  $\theta_{CO}$  at any moment because the QMS was measuring the partial pressure and there was some lag due to the pumping speed for CO in the UHV chamber.

On the (2×1)-O adlayer at 300 K or below, CO also adsorbed intact and inserted into the adlayer forming a (2×2)-2O+CO adlayer. $^{27,29}$  Although at higher temperatures CO would be oxidized, removing  $O_{ad}$ , for  $T_s$  < 300 K, the reaction was not significant. $^9$  RAIRS taken after exposure of (2×1)-O to CO is shown in Figure 3A, and only a single absorption peak, corresponding to a C–O stretching mode, was observed at 2088 cm $^{-1}$ . Unlike CO on Rh(111), there was no shift in the peak location and the intensity monotonically increased with exposure, and rapidly saturated. This straightforward relationship between CO exposure and RAIRS intensity suggests that the factors that gave CO on Rh(111) the complex behaviors were not present on the oxygenated surface, likely because, although still metallic,  $O_{ad}$  reduced the availability of electron density to the CO, and contributions to CO–Rh orbitals aside from the surface–adsorbate bond did not occur.

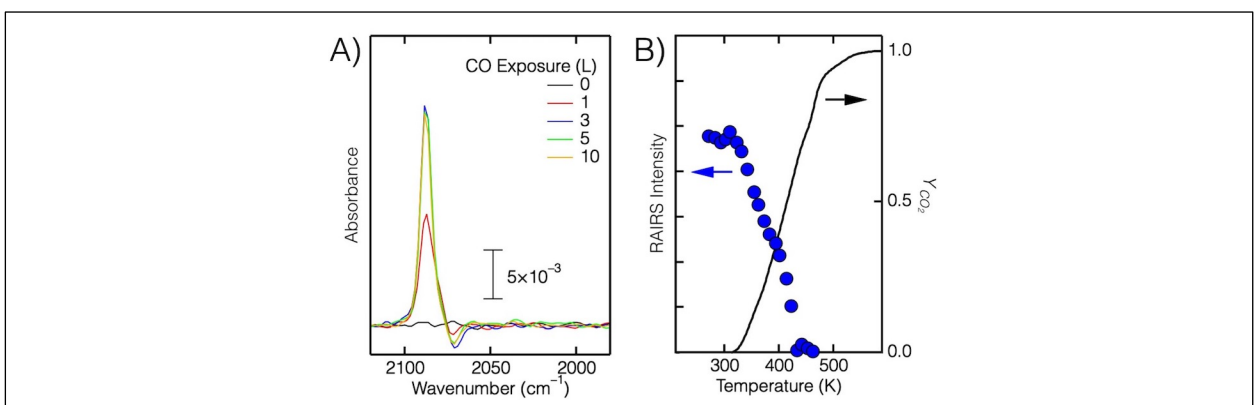


Figure 3: CO on  $(2\times1)$ -O/Rh(111). A) RAIRS taken during CO exposure for  $T_{exp}$  = 300 K showing single C–O stretch absorption peak that rapidly saturated. B) IRRAS intensity (left) for CO on  $(2\times1)$ -O during TPD experiment (blue circles) and  $Y_{CO}$  from TPD data (right), the integral of the CO<sub>2</sub> desorption peak.

However, IR spectra collected during the TPD experiment showed a transition not present for CO/Rh(111). As shown in Figure 4A, and 4B around 300 K (the CO exposure temperature) the absorption peak shifted from 2088 cm<sup>-1</sup> to 2068 cm<sup>-1</sup>, the same frequency observed for CO on clean Rh(111). In addition, there was no absorption corresponding to CO binding at bridge sites, which was evident on Rh(111) in Figures 4C and 4D around 1850 cm<sup>-1</sup>. This shift occurred at the onset of CO oxidation to CO<sub>2</sub>, as indicated by the appearance of CO<sub>2</sub> in the TPD, shown in Figure 3B (right axis, black trace). After a narrow window of coexistence, only the 2068 cm<sup>-1</sup> peak was observed, and then as  $T_s$  increased, the RAIRS intensity steadily decreased, as shown in Figure 3B, left axis. The fact that the shift in IR absorption and desorption of CO<sub>2</sub> occurred simultaneously indicated that the reactive CO fingerprint was the 2068 cm<sup>-1</sup> mode. However, it is unclear at this point if this was due to a shift in binding site or from another factor. Figure 4 compares how the IR spectra of oxygenated to clean Rh(111) evolved with  $T_s$  and  $\theta_{CO}$ . As previously discussed, on Rh(111), CO desorption caused an increase in the RAIRS intensity although  $\theta_{CO}$  decreased, shown in Figures 4C and 4D. On the

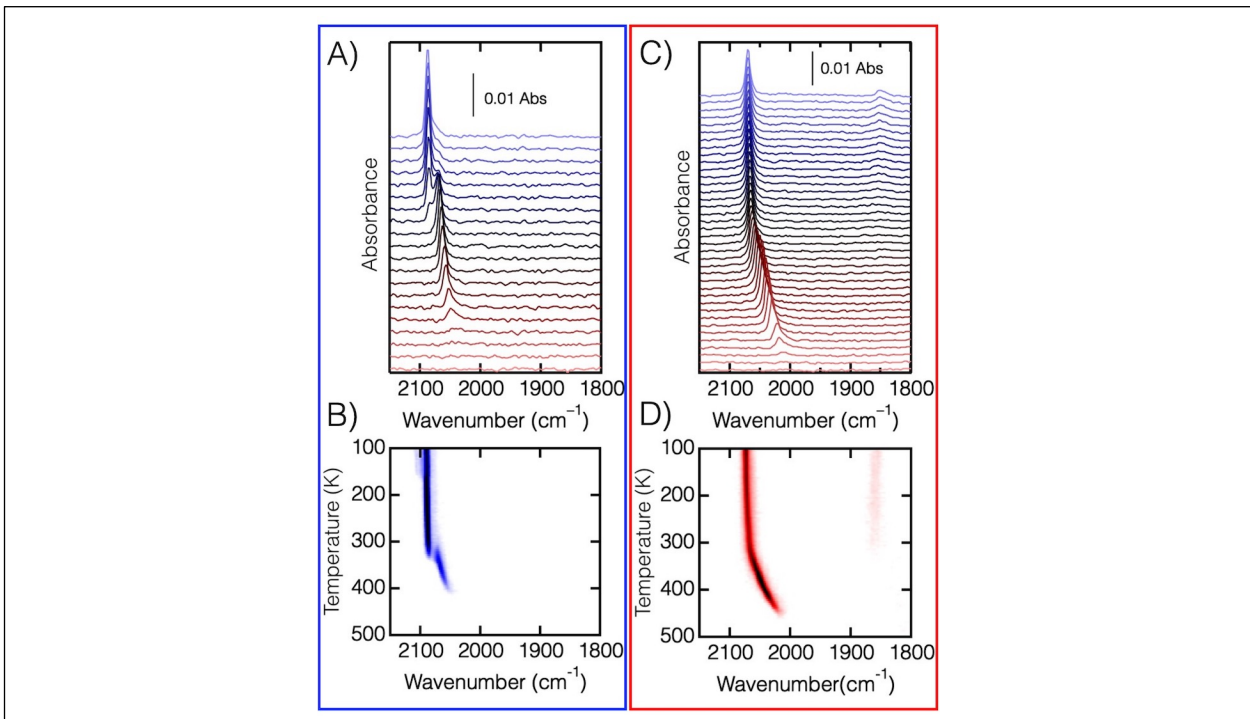


Figure 4: A) (top) IR spectra taken during TPD experiment for an initial preparation of 30 L CO exposure at  $T_{exp} = 300$  K on (2×1)-O/Rh(111). The transition from a single peak at 2088 cm<sup>-1</sup> to 2068 cm<sup>-1</sup>, with a limited coexistence around 300 K. B) 2-D plot to highlight the peak shift. C) IR spectra for 0.75 ML CO on Rh(111) during TPD ramp and D) 2-D plot to highlight smooth shift in maxima.

oxygenated surface, shown in Figures 4A and 4B, the RAIRS peak was unchanged until the transition to 2068 cm<sup>-1</sup> near 300 K, and thereafter followed the same path as CO on Rh(111) without  $O_{ad}$ . However, instead of merely desorbing, the CO was being oxidized to  $CO_2$ . This suggests that CO oxidation occurred along the desorption pathway, as the chemical state was the same, as indicated by the C–O absorption peak location. However, the steady decrease in RAIRS intensity with  $\theta_{CO}$  shows that RAIRS intensity was proportional to the CO coverage on the oxygenated surface.

## IV. Summary and Conclusion

The intensity and location of the C–O stretch from the surface IR spectra of CO on Rh(111) and (2×1)-O/Rh(111) clearly depended on the surface temperature. On clean Rh(111), CO deposited at 300 K yielded a sharp C–O absorption peak between 2072 cm<sup>-</sup>

¹ and 2086 cm⁻¹, characteristic of adsorption on Rh atop sites, and a significantly smaller, broad peak near 1850 cm⁻¹ corresponding to binding on Rh bridge sites. Upon heating in a TPD experiment, the atop C–O stretch first increased in intensity, before decreasing and redshifting as  $\theta_{CO}$  decreased. Alternatively, RAIRS of CO on (2×1)-O/Rh(111) gave only the atop C–O stretch feature initially at 2088.5 cm⁻¹, which shifted to ≈2070 cm⁻¹ with heating and the progress of CO oxidation until it too diminished in intensity and redshifted as seen on clean Rh(111). These results show that quantitative RAIRS requires more than only peak intensity . Furthermore, because the CO chemical environment was the same whether Oad was present or not, CO oxidation occurs along the desorption pathway. These results show the subtle interplay between coverage and temperature for CO oxidation on rhodium surfaces.

### **Author Declarations**

The authors have no conflicts to disclose

Supplemental Materials

# **Acknowledgments**

We wish to acknowledge support from the National Science Foundation through award CHE-1800291. E.A. Jamka thanks Loyola University Chicago for support through the Teaching Scholars Program during this work.

### **Data Availability**

Data available on request from the authors

#### References

- 1. H. J. Freund and G. A. Somorjai, Catal. Lett. **145**, 1-2 (2015).
- 2. J. F. Weaver, Chemical Reviews **113**, 4164-4215 (2013).
- 3. R. Ye, T. J. Hurlburt, K. Sabyrov, S. Alayoglu and G. A. Somorjai, Proc. Natl. Acad. Sci. **113**, 5159-5166 (2016).
- 4. S. Schwegmann, H. Over, V. DeRenzi and G. Ertl, Surf. Sci. **375**, 91-106 (1997).
- 5. M. M. Montemore, M. A. van Spronsen, R. J. Madix and C. M. Friend, Chemical Reviews **118**, 2816-2862 (2018).
- 6. G. B. Park, T. N. Kitsopoulos, D. Borodin, K. Golibrzuch, J. Neugebohren, D. J. Auerbach, C. T. Campbell and A. M. Wodtke, Nature Reviews Chemistry **3**, 723-732 (2019).
- 7. J. Neugebohren, D. Borodin, H. W. Hahn, J. Altschäffel, A. Kandratsenka, D. J. Auerbach, C. T. Campbell, D. Schwarzer, D. J. Harding, A. M. Wodtke and T. N. Kitsopoulos, Nature **558**, 280-283 (2018).
- 8. L. S. Brown and S. J. Sibener, The Journal of Chemical Physics **90**, 2807-2815 (1989).
- 9. M. E. Turano, R. G. Farber, G. Hildebrandt and D. R. Killelea, Surf. Sci. **695**, 121573 (2020).
- 10. R. G. Farber, M. E. Turano and D. R. Killelea, ACS Catal. **8**, 11483-11490 (2018).
- 11. M. J. P. Hopstaken and J. W. Niemantsverdriet, J. Chem. Phys. **113**, 5457-5465 (2000).
- 12. H. Hopster, H. Ibach and G. Comsa, J. Catal. **46**, 37 48 (1977).
- 13. A. J. Jaworowski, A. Beutler, F. Strisland, R. Nyholm, B. Setlik, D. Heskett and J. N. Andersen, Surf. Sci. **431**, 33-41 (1999).

- 14. F. Zhang, L. Pan, T. Li, J. T. Diulus, A. Asthagiri and J. F. Weaver, J. Phys. Chem. C **118**, 28647-28661 (2014).
- 15. M. M. M. Jansen, F. J. E. Scheijen, J. Ashley, B. E. Nieuwenhuys and J. W. Niemantsverdriet, Catalysis Today **154**, 53-60 (2010).
- 16. G. Krenn, I. Bako and R. Schennach, The Journal of Chemical Physics **124**, 144703 (2006).
- 17. J. D. Krooswyk, J. Yin, A. L. Asunskis, X. F. Hu and M. Trenary, Chem. Phys. Lett. **593**, 204-208 (2014).
- 18. L. S. Zhou, A. Kandratsenka, C. T. Campbell, A. M. Wodtke and H. Guo, Angew. Chem. Int. Ed. **58**, 6916-6920 (2019).
- 19. G. B. Park, B. C. Kruger, D. Borodin, T. N. Kitsopoulos and A. M. Wodtke, Reports on Progress in Physics **82**, 09640 (2019).
- 20. Z. Liang, T. Li, M. Kim, A. Asthagiri and J. F. Weaver, Science **356**, 298-301 (2017).
- 21. C. Badan, R. G. Farber, Y. Heyrich, M. T. M. Koper, D. R. Killelea and L. B. F. Juurlink, J. Phys. Chem. C **120**, 22927-22935 (2016).
- 22. M. E. Turano, E. A. Jamka, M. Z. Gillum, K. D. Gibson, R. G. Farber, W. Walkosz, S. J. Sibener, R. A. Rosenberg and D. R. Killelea, J. Phys. Chem. Lett. **12**, 5844-5849 (2021).
- 23. R. G. Farber, M. E. Turano, E. C. N. Oskorep, N. T. Wands, E. V. Iski and D. R. Killelea, J. Phys. Chem. C **121**, 10470-10475 (2017).
- 24. J. Derouin, R. G. Farber and D. R. Killelea, J. Phys. Chem. C **119**, 14748-14755 (2015).
- 25. A. L. Gerrard and J. F. Weaver, The Journal of Chemical Physics **123**, 224703 (2005).
- 26. C. M. Kruppe, J. D. Krooswyk and M. Trenary, J. Phys. Chem. C **121**, 9361-9369 (2017).

- 27. D. Curulla, R. Linke, A. Clotet, J. M. Ricart and J. W. Niemantsverdriet, Chem. Phys. Lett. **354**, 503-507 (2002).
- 28. R. Linke, D. Curulla, M. J. P. Hopstaken and J. W. Niemantsverdriet, The Journal of Chemical Physics **115**, 8209-8216 (2001).
- 29. A. C. Kizilkaya, J. M. Gracia and J. W. Niemantsverdriet, J. Phys. Chem. C **114**, 21672-21680 (2010).
- 30. K. D. Gibson, J. I. Colonell and S. J. Sibener, Surf. Sci. **343**, L1151-L1155 (1995).
- 31. P. A. Thiel, J. T. Yates and W. H. Weinberg, Surf. Sci. 82, 22-44 (1979).
- 32. P. A. Thiel, E. D. Williams, J. T. Yates and W. H. Weinberg, Surf. Sci. **84**, 54-64 (1979).
- 33. A. Föhlisch, M. Nyberg, P. Bennich, L. Triguero, J. Hasselström, O. Karis, L. G. M. Pettersson and A. Nilsson, The Journal of Chemical Physics **112**, 1946-1958 (2000).
- 34. G. A. Somorjai and Y. Li, *Introduction to Surface Chemistry and Catalysis*, 2nd ed. (John Wiley & Sons, Inc., Hoboken, NJ, 2010).
- 35. C. M. Gunathunge, J. Li, X. Li and M. M. Waegele, ACS Catal. **10**, 11700-11711 (2020).

## **Early Career Bios**

Elizabeth A. Jamka was born and raised in the Chicagoland suburbs. She graduated from Elmhurst University (formally Elmhurst College) with Honors in 2015. At Loyola University Chicago she has won Teaching Assistant of the year award in 2020 and was a Teaching Scholars Fellow for the 2021-2022 academic year. She is an active alumni member and chapter advisor for Alpha Phi Omega, a co-ed service fraternity, serving in the organization since her time at Elmhurst University.

Maxwell Z. Gillum is a 3<sup>rd</sup> year graduate student currently working towards his PhD at Loyola University Chicago. He completed his undergraduate degree at James Madison University in 2019, where he also worked in an ultra-high vacuum laboratory. Originally from Virginia, Maxwell loves to hike and be outside. In the future, he has plans of becoming a college professor to continue doing ultra-high vacuum catalysis research.



Christina N. Grytsyshyn-Giger is graduating from Loyola University Chicago in May 2022 with her Bachelor of Science in Chemistry and a minor in Mathematics. Christina was born and raised in Chicago, but also lived in Ukraine for a few years. She has worked in Killelea lab since 2020. And will be taking a gap year after graduation before pursuing graduate school for her PhD.



Faith J. Lewis will be graduating from Loyola University Chicago in 2022 with her Bachelor of Science in Chemistry and will continue at LUC to complete her Master of Science Chemistry expected May 2023. She was awarded the Chair Recognition Award in 2022 as a graduating senior. She has been a part of the Killelea lab since early 2019. After graduation she plans on working in industry before deciding to continue with graduate school.

